

A Robust Algorithm for Eye-Diagram Analysis

Jeffrey A. Jargon, *Senior Member, IEEE*, C. M. “Jack” Wang, and Paul D. Hale, *Senior Member, IEEE*

Abstract—We present a new method for analyzing eye diagrams that always provides a unique solution by making use of a robust, least-median-of-squares (LMS) location estimator. In contrast to commonly used histogram techniques, the LMS procedure is insensitive to outliers and data distributions. Our motivation for developing this algorithm is to create an independent, benchmark method that is both amenable to a thorough uncertainty analysis and can function as a comparison tool since no standardized industry algorithms currently exist. Utilizing this technique, we calculate the fundamental parameters of an eye diagram, namely the one and zero levels, and the time and amplitude crossings. With these parameters determined, we can derive various performance metrics, such as extinction ratio and root-mean-square jitter, and perform eye-mask alignment. In addition to describing our algorithm in detail, we compare results computed with this method to those of a commercial oscilloscope, and obtain excellent agreement. Finally, we suggest new definitions of eye height and eye width that are more robust than those that are commonly used.

Index Terms—Extinction ratio, eye diagram, least-median-of-squares (LMS) location estimator, robust statistics.

I. INTRODUCTION

EYE diagrams are multivalued displays used for assessing the quality of high-speed digital signals [1]. They are usually constructed by applying a data waveform to the input of a sampling oscilloscope, and then overlapping all possible one-zero combinations on the instrument’s display so as to span three intervals, as shown in Fig. 1. This is accomplished by triggering the oscilloscope at the data-clock frequency and setting the display for infinite persistence, so that previous waveforms remain on the screen while subsequent ones are added.

Eye diagram measurements have a huge economic impact on the optical and electrical communications industries. With cost pressures driving manufacturers to create products that just meet specifications, the ability to make accurate and repeatable measurements is becoming more important. Conflicts may arise between component manufacturers and their customers when different test equipment leads to measurement inconsistencies. These discrepancies can be attributed to both software and hardware differences. Although work is being done to address hardware deficiencies [2], [3], we focus our attention on algorithmic issues that can be implemented in software.

Manuscript received September 17, 2007; revised December 31, 2008. Current version published January 28, 2009. This work is a contribution of the National Institute of Standards and Technology and is not subject to copyright in the United States.

J. A. Jargon and P. D. Hale are with the Optoelectronics Division, National Institute of Standards and Technology, Boulder, CO 80305-3328 USA (e-mail: jargon@boulder.nist.gov; hale@boulder.nist.gov).

C. M. J. Wang Statistical Engineering Division, National Institute of Standards and Technology Boulder, CO 80305-3328 USA (e-mail: jwang@boulder.nist.gov).

Digital Object Identifier 10.1109/JLT.2008.917313

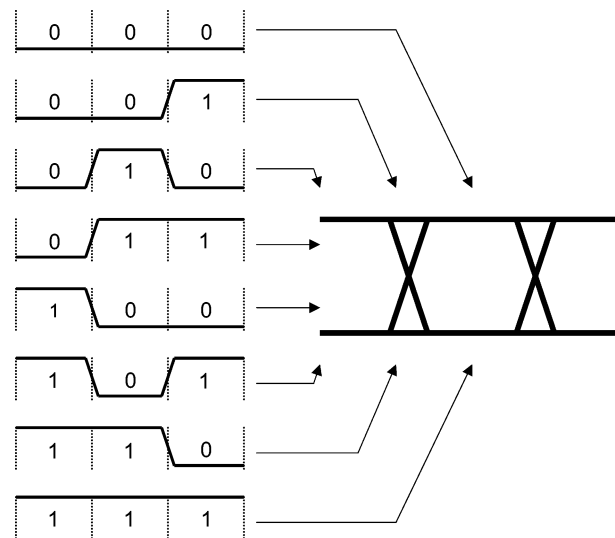


Fig. 1. Eye diagram is constructed by overlapping all possible one-zero combinations on an instrument’s display.

Because eye diagrams are an aggregate representation of one-zero combinations, a histogram analysis, along with an iterative algorithm, is usually used to derive the fundamental parameters of the eye, namely the one level, zero level, crossing times, and crossing amplitudes [4], [5]. Using these calculated parameters, shown in Fig. 2, we can perform eye mask alignment and compute various performance metrics, such as extinction ratio, eye height, eye width, Q factor, and jitter.

The problem with histograms is that the solutions vary with the chosen number of bins and bin sizes, and, thus, they yield no unique answer. Furthermore, the values of the performance metrics differ depending upon whether the mean, mode, or median of the histogram is utilized. The IEEE Standard on Transitions, Pulses, and Related Waveforms [6] recommends using the mode or mean of a histogram, both of which depend on the distribution of the data. This is particularly important with respect to eye patterns, where the distribution is often not symmetric. For example, when a histogram technique was used to calculate the extinction ratio from the eye diagram shown in Fig. 2, we discovered that the computed value was almost 3 dB, or two times, larger when using the mode as compared to the median. Finally, a large number of measurements might be required to obtain stable histograms.

With histogram methods being inherently sensitive to binning and data distributions, and because oscilloscope manufacturers’ algorithms are proprietary, it is difficult if not impossible to directly compare or verify their algorithms. Thus, we propose an alternate method for analyzing an eye diagram that 1) always provides a unique solution, and 2) is fully disclosed in the public literature. Specifically, we make use of a least median of squares

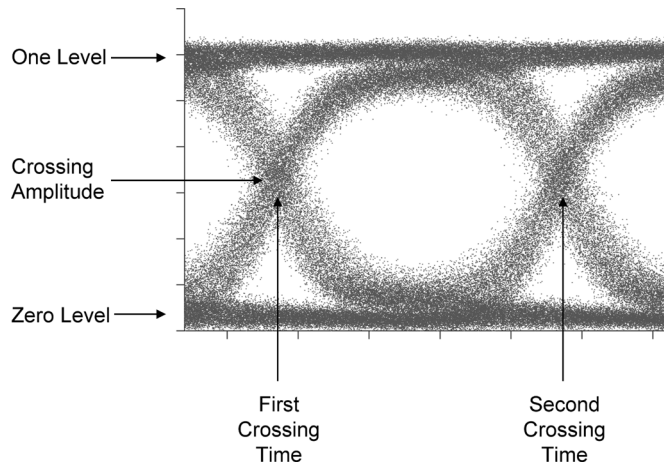


Fig. 2. Fundamental properties of an eye diagram.

(LMS) location estimator [7] that seeks a “collective” mode in the data. This method can tolerate up to 50% of contaminated data, making it very robust against outliers. In the following sections, we describe the technique in detail, compare results computed with this method to those of a commercial oscilloscope, and suggest new definitions of eye height and eye width that are more robust than those that are commonly used. In the Appendix, we include the code that was implemented for analyzing eye diagrams with the LMS algorithm.

The LMS algorithm is intended primarily for determining the fundamental parameters of an eye diagram, which can then be used to derive various performance metrics and perform eye-mask alignment. Although we do present a technique for calculating root-mean-square jitter, the subjects of deterministic jitter and dual-Dirac model-fitting techniques are not explored in this paper.

We wish to point out that the proposed algorithm is not intended to replace existing histogram methods in commercial oscilloscopes. Rather, its purpose is twofold: 1) to serve as an independent, benchmark method that is amenable to a thorough uncertainty analysis, and 2) to function as a comparison tool since no standardized industry algorithms currently exist.

Note that data waveforms can take the form of return-to-zero (RZ) and non-return-to-zero (NRZ), and can be either binary or multilevel. In this paper, we consider NRZ, binary-level data.

II. ALGORITHM

In this section we describe our algorithm for analyzing an eye diagram. First, we derive the fundamental parameters of the eye, and then using these calculated parameters, we show how to calculate various performance metrics, including extinction ratio, eye height, eye width, Q factor, and jitter. Fig. 3 is a flowchart summarizing the algorithm.

A. Calculating the Fundamental Parameters

We begin by deriving the fundamental parameters of the eye, namely the one level, zero level, crossing times, and crossing amplitudes.

1) *Fundamental Parameters—Step 1:* In order to determine the one and zero levels, we begin by grouping the eye dia-

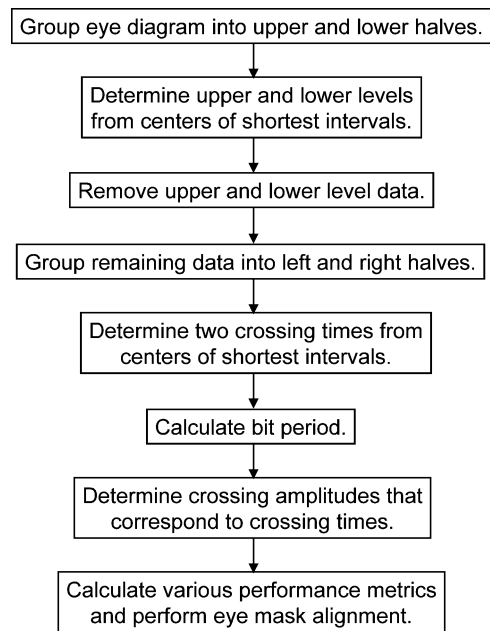


Fig. 3. Flowchart of the proposed algorithm for analyzing an eye diagram.

gram data based on amplitude (Y-axis) into upper and lower halves. This is done with a K-Means algorithm for clustering objects into groups [8]. The algorithm works by first randomly partitioning the data into k initial sets (in our case $k = 2$). Next, the mean point, or centroid, of each set is calculated. A new partition is constructed by associating each point with the closest centroid. Then, the centroids are recalculated for the new clusters, and the algorithm repeats by alternating between the previous two steps until convergence occurs, which is accomplished when the points no longer switch clusters, or alternatively, the calculated centroids no longer change.

2) *Fundamental Parameters—Step 2:* Next, we determine the upper and lower levels from the centers of their respective shortest intervals. For the upper half, the shortest interval that contains 50% of the data is determined. This is motivated by the need to find a “mode” without using the histogram method. The idea is that, instead of locating a (single-number) mode, we look for a concentration, or a “collective” mode, in the data. We use the “50% of the data” criterion for concentration. The midpoint of this shortest interval, denoted by \bar{v}_1 , can then be considered as a mode estimator and is used to estimate the one level. It has been shown [7] that the mode so obtained is also a least median of squares (LMS) estimator for the data. Let y_1, \dots, y_n be the data. Then the LMS estimator for $y_i, i = 1, \dots, n$, denoted by \tilde{y} , is the solution of

$$\min_{\tilde{y}} \text{median} [(y_i - \tilde{y})^2, i = 1, \dots, n].$$

The LMS estimator can tolerate up to 50% of contaminated data; making it very robust against outliers. In contrast, the arithmetic mean $\bar{y} = \sum_{i=1}^n y_i/n$, which is the solution of

$$\min_{\bar{y}} \sum_{i=1}^n (y_i - \bar{y})^2$$

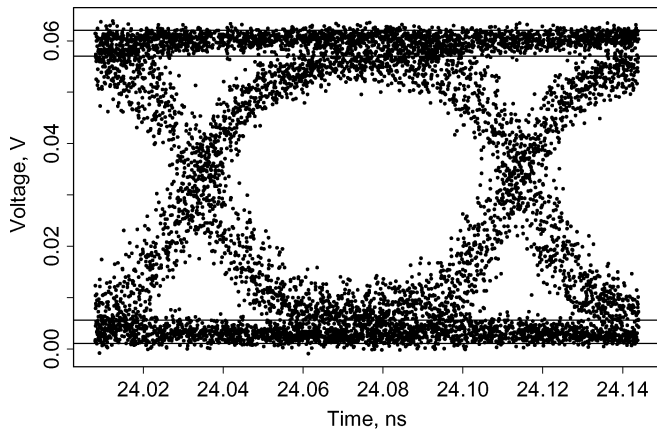


Fig. 4. Shortest intervals that contain 50% of the upper and lower halves.

cannot tolerate any outliers; a single aberrant value can cause \bar{y} to give an arbitrarily bad result.

As an aside, another mode estimator based on the shortest interval, called the *shorth* estimator [7], is the arithmetic mean of the data in the interval. Both the LMS and the shorth estimators produce practically identical results for applications in this paper. Here, we use the LMS estimator since it is slightly easier to calculate, although we have used the shorth estimator for a similar topic [9].

The shortest interval is the interval that produces the smallest of the following differences:

$$y_{(h)} - y_{(1)}, y_{(h+1)} - y_{(2)}, \dots, y_{(n)} - y_{(n-h+1)}$$

where $h = \lceil n/2 \rceil + 1$, $\lceil x \rceil$ stands for the greatest integer less than or equal to x , and $y_{(1)} \leq y_{(2)} \leq \dots \leq y_{(n)}$ are the ordered observations.

As a simple illustration, suppose $n = 11$ and the ordered observations are 10, 45, 50, 53, 56, 58, 60, 62, 63, 65, 75. Then $h = 6$ and the smallest of the differences: 58-10, 60-45, 62-50, 63-53, 65-56, 75-58, is 9, which corresponds to the interval (56, 65). The midpoint of this interval, 60.5, is the LMS estimate for these eleven observations. If we assume the lowest-ordered observation is an outlier and we exclude it, the LMS estimate is still 60.5. Contrast this with other common methods. The mean of the eleven observations is 54.3, whereas it climbs to 58.7 when the outlier is excluded. Likewise, the median is 58 for the eleven observations, and 59 when the outlier is left out.

Similar to that of the upper half, the shortest interval that contains 50% of the data is determined for the lower cluster. The midpoint of the shortest interval, denoted by \bar{v}_0 , corresponds to the zero level. Fig. 4 illustrates the shortest intervals for both the upper and lower halves.

3) *Fundamental Parameters—Step 3:* With the upper and lower levels determined, we now focus our attention on the crossing times. First, we remove upper and lower level data by calculating $v_{25} = \bar{v}_0 + 0.25(\bar{v}_1 - \bar{v}_0)$ and $v_{75} = \bar{v}_1 - 0.25(\bar{v}_1 - \bar{v}_0)$. Eliminate all of the data that lie outside of the range (v_{25}, v_{75}) , as illustrated in Fig. 5.

4) *Fundamental Parameters—Step 4:* In order to determine the two crossing times, we group the remaining data based on

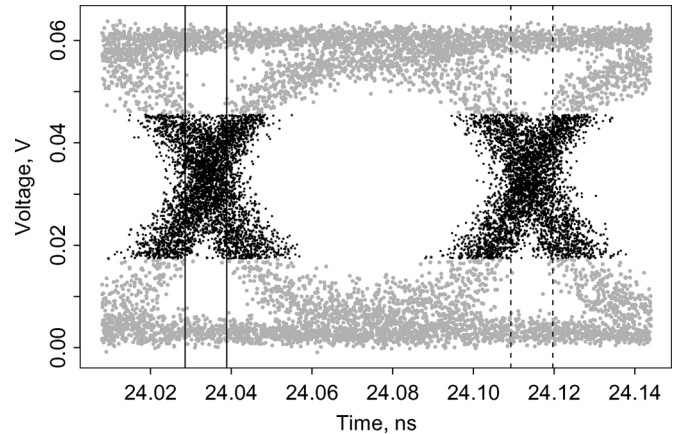


Fig. 5. Gray points are not used in the calculation of crossing times. The vertical lines are the shortest intervals that contain 50% of the left and right halves.

time (X-axis) into left and right halves using the K-means algorithm.

5) *Fundamental Parameters—Step 5:* Next, we determine the two crossing times from the centers of their respective shortest intervals. For the left half, the shortest interval that contains 50% of the data (on X-axis) is determined. This interval is indicated by the two solid vertical lines in Fig. 5. Once this interval is determined, compute the midpoint of the interval. This value, denoted by \bar{t}_1 , corresponds to the first crossing time.

Likewise, the shortest interval that contains 50% of the data is determined for the right half. It is indicated by the two dashed vertical lines in Fig. 5. Once again, compute the midpoint \bar{t}_2 . This value corresponds to the second crossing time.

6) *Fundamental Parameters—Step 6:* Finally, we compute the crossing amplitudes. Start by calculating the bit period T_B as follows:

$$T_B = \bar{t}_2 - \bar{t}_1.$$

Using the left half of the data that were clustered in step 4, determine the first crossing amplitude by considering only those data that lie within a small range around \bar{t}_1 , such as $\bar{t}_1 \pm 0.01T_B$, and compute the mean \bar{v}_{c1} . This value corresponds to the first crossing amplitude.

Likewise, using the right half of the data that were clustered in step 4, determine the second crossing amplitude by considering only those data that lie within the range $\bar{t}_2 \pm 0.01T_B$, and compute the mean \bar{v}_{c2} . This value corresponds to the second crossing amplitude. Fig. 6 illustrates both crossing amplitudes.

At this point, we have determined the fundamental parameters of the eye, namely the one level \bar{v}_1 , zero level \bar{v}_0 , crossing times \bar{t}_1 and \bar{t}_2 , and crossing amplitudes \bar{v}_{c1} and \bar{v}_{c2} . Using these calculated parameters, we can now perform mask tests and compute various performance metrics.

B. Calculating Extinction Ratio

Next, we calculate the extinction ratio ER, which is defined as the ratio of the average power used to transmit a logic level “1” to the average power used to transmit a logic level “0” [10].

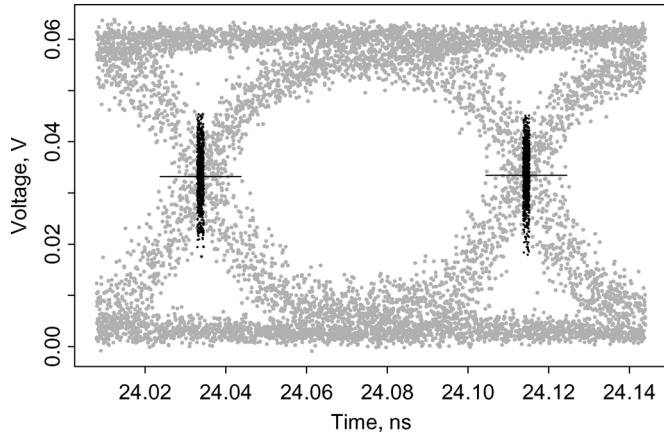


Fig. 6. Data used to calculate crossing amplitudes. The horizontal lines are the left and right crossing amplitudes.

First, calculate the central point of the eye diagram t_c as follows:

$$t_c = \frac{\bar{t}_1 + \bar{t}_2}{2}.$$

Many international standards [11]–[15] specify extinction ratio to be computed from the mean of the data located in the central 20% of the eye diagram. Thus, the time span covers $t_c \pm 0.1T_B$.

Next, separate the data located in the central 20% of the eye diagram into top and bottom halves. This is done by using the value $(\bar{v}_0 + \bar{v}_1)/2$ as the horizontal separator. For each cluster, calculate the means \bar{v}_{high} and \bar{v}_{low} , and standard deviations s_{high} and s_{low} . See Fig. 8 for a graphical illustration.

Finally, calculate the extinction ratio as follows:

$$\text{ER} = \frac{\bar{v}_{\text{high}}}{\bar{v}_{\text{low}}}.$$

C. Calculating RMS Jitter

Next, we calculate the root-mean-square (RMS) jitter, which is usually defined as the standard deviation of the time data calculated in a narrow window surrounding the crossing amplitude [1], [4]. See Fig. 7 for a graphic illustration.

Using the left half of the data that was clustered in Section II-A4, determine the RMS jitter at the first crossing amplitude by considering only the data that lie within the range $\bar{v}_{c_1} \pm 0.01(\bar{v}_1 - \bar{v}_0)$, and compute the standard deviation s_{t_1} . This value corresponds to the RMS jitter at the first crossing amplitude.

Using the right half of the data that were clustered in Section II-A4, determine the RMS jitter at the second crossing amplitude by considering only the data that lie within the range $\bar{v}_{c_2} \pm 0.01(\bar{v}_1 - \bar{v}_0)$, and compute the standard deviation s_{t_2} . This value corresponds to the RMS jitter at the second crossing amplitude.

Calculate the overall RMS jitter as follows:

$$s_t = \frac{s_{t_1} + s_{t_2}}{2}.$$

Note that we make use of both crossing points in our determination of RMS jitter. Normally, in an eye diagram, one crossing

point should essentially be the duplicate of the other. However, when the data are random or the pattern is long, not all combinations may be present in both sides of the eye. Thus, utilizing the two crossing points to derive the RMS jitter provides a more robust estimation. As far as we know, commercial solutions have not yet taken advantage of this improvement.

D. Calculating Eye Height, Eye Width, and Q Factor

Three other commonly computed performance metrics are eye height, eye width, and Q factor [1], [4]. They are commonly defined as follows:

$$\begin{aligned} \text{eyeheight} &= (\bar{v}_{\text{high}} - 3s_{\text{high}}) - (\bar{v}_{\text{low}} + 3s_{\text{low}}) \\ \text{eyewidth} &= (\bar{t}_2 - 3s_{t_2}) - (\bar{t}_1 + 3s_{t_1}) \end{aligned}$$

and

$$\text{Q factor} = \frac{\bar{v}_{\text{high}} - \bar{v}_{\text{low}}}{s_{\text{high}} + s_{\text{low}}}.$$

III. COMPARISONS

In this section, we compare results computed from our method, described in the previous section, to those provided by a commercial oscilloscope. This allows us to verify our algorithm, and lay the foundation for suggesting further improvements that cannot be accomplished by use of a traditional histogram approach. We performed our comparison on two measurement setups, both of which used a pattern generator that produced a $2^{15} - 1$ pseudo-random binary sequence (PRBS) at 10 Gbps and a commercial, equivalent-time sampling oscilloscope. This oscilloscope is specially equipped with a prescaler to accommodate the 10 GHz trigger signal.

In the first setup, we used a distributed feedback (DFB) laser operating at 1550 nm in conjunction with an external Mach-Zender modulator. The digital signal from the pattern generator was amplified prior to being fed into the modulator. The output of the modulator was connected to the oscilloscope’s optical input, which included a built-in, low-pass filter to produce a SDH/SONET reference receiver. Fig. 9 illustrates this arrangement. Typical measurements of these waveforms were used as the example in Figs. 2–8. To evaluate our method, we saved 30 waveforms, each containing 4096 points, from the oscilloscope, and used our algorithm to compute the extinction ratio, eye height, eye width, and RMS jitter. We then repeated this 30 times and calculated the mean and standard deviation of each of the four parameters. Likewise, we took 30 repeated readings from the oscilloscope, and performed the same calculations. Table I summarizes the results, where the standard deviations are in parentheses. The two algorithms agree remarkably well, with the largest discrepancy being a 1.5% difference in extinction ratio.

In the second setup, we used a directly-modulated DFB laser operating at 1550 nm, shown in Fig. 10. This time, the output of the laser was directly connected to the oscilloscope’s optical input, with the built-in, low-pass filter turned off. We did this in order to illustrate a pathological case. Once again, we saved 30 waveforms from the oscilloscope, computed the extinction ratio, eye height, eye width, and RMS jitter, and then compared

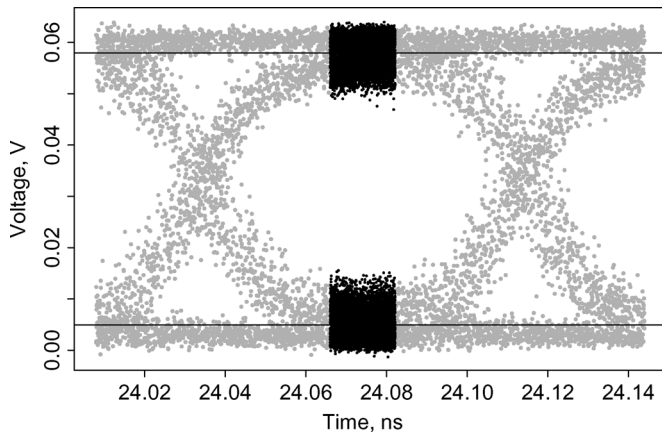


Fig. 7. Data used to calculate extinction ratio. The horizontal lines are the calculated values of \bar{v}_{high} and \bar{v}_{low} .

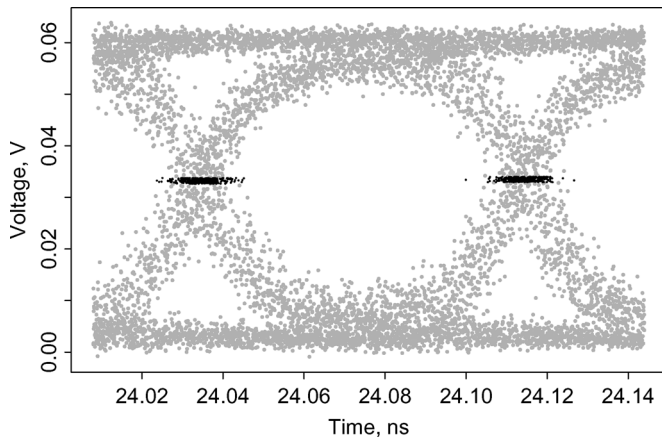


Fig. 8. Data used to calculate the RMS jitter values.

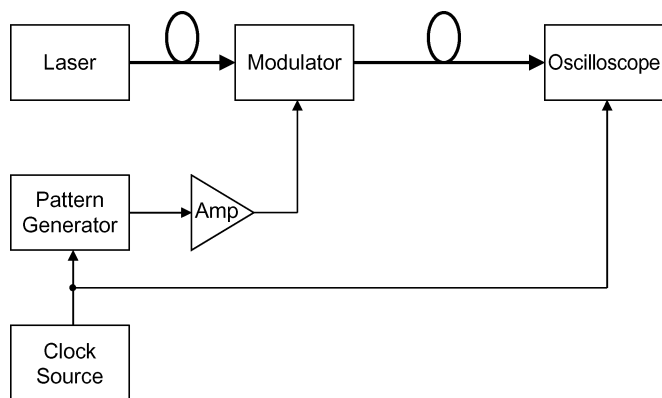


Fig. 9. Measurement setup using an external modulator.

TABLE I
COMPARISON FOR THE FIRST MEASUREMENT SETUP

Parameter	Proposed algorithm	Oscilloscope algorithm
Extinction ratio (dB)	12.22 (0.04)	12.40 (0.03)
Eye height (mW)	1.052 (0.005)	1.049 (0.002)
RMS jitter (ps)	3.52 (0.05)	3.52 (0.07)
Eye width (ps)	79.2 (1.3)	78.8 (0.4)

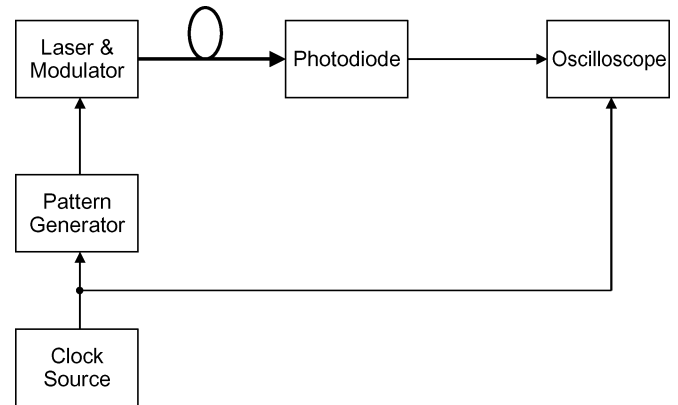


Fig. 10. Measurement setup using direct modulation.

TABLE II
COMPARISON FOR THE SECOND MEASUREMENT SETUP

Parameter	Proposed algorithm	Oscilloscope algorithm
Extinction ratio (dB)	4.60 (0.01)	4.64 (0.01)
Eye height (mW)	0.131 (0.002)	0.131 (0.002)
RMS jitter (ps)	3.03 (0.09)	3.04 (0.07)
Eye width (ps)	81.6 (0.6)	81.3 (0.5)

the mean values of the 30 repeats to those provided by the oscilloscope. Table II summarizes the results. In this case, the agreement between the two algorithms is even better.

We also used one set of 30 waveforms from the data in the first setup to examine the relationship between the computed parameters and the number of waveforms used in the calculation. Using the LMS algorithm, we started with one waveform, calculated the parameters, and repeated this process while incrementing the number of included waveforms until we reached a total of 30. Since the results for all four parameters exhibited similar behavior, we only show the extinction ratio in Fig. 11. In contrast, the oscilloscope we used does not report an extinction ratio until at least one pixel on the display has been hit at least 15 times. The manufacturer states that 20 or more waveforms may be required to achieve this density; however, with the 4096 points per waveform that we acquired, usually only 6 or 7 waveforms were measured before the extinction ratio was displayed. Fig. 11 shows the values of extinction ratio reported by the oscilloscope as a function of the number of waveforms included in the calculation. Without being able to perform a direct comparison, it appears that the two algorithms converge at similar rates.

IV. DISCUSSION

In this paper, we have presented an algorithm for analyzing an eye diagram. The algorithm relies on a robust location estimation method to calculate the fundamental parameters of the eye diagram, which does not assume a maximum level of closure. The fundamental parameters and various parameter-derived performance metrics of the eye diagram calculated by use of the proposed algorithm are in good agreement with those obtained from a commercial oscilloscope.

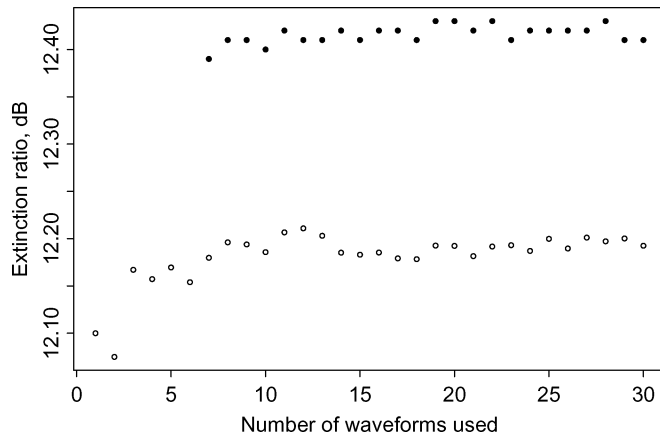


Fig. 11. Calculated values of extinction ratio as a function of number of waveforms used in the calculation. The solid circles represent values calculated with the oscilloscope algorithm, and the hollow circles represent those calculated with the proposed LMS algorithm.

Performance metrics, such as the extinction ratio, RMS jitter, eye height, and eye width, are obtained based on the means and standard deviations of the data located in certain areas of the eye. Since both the mean and standard deviation are not robust, performance metrics based on them may not work well if there are outliers in those areas. To illustrate, consider the second measurement setup discussed in Section III. Fig. 12 displays the sections of the eye that were used to calculate the extinction ratio and eye height. The two solid lines are $(\bar{v}_{\text{high}} - 3s_{\text{high}})$ and $(\bar{v}_{\text{low}} + 3s_{\text{low}})$, respectively. The distance between these two lines, 9.2 mV, is used to estimate eye height. Obviously, this is not a good estimate; the top solid line underestimates the “lower” limit of the upper cluster due to the presence of “abnormal” measurements. A more robust way for computing the limits in this situation is to use the percentiles of the data. In a Gaussian distribution, $\mu - 3\sigma$ represents the 0.13 percentile of the distribution. Thus, we can use the 0.13 percentile of the data in the upper cluster as the lower limit of the cluster, which is the top dashed line in Fig. 12. Similarly, the bottom dashed line is the 99.87 percentile of the data in the lower cluster. The difference between the two dashed lines, 10.2 mV, is a more reasonable estimate for eye height. The same approach can also be used in the calculation of eye width.

It is also always a good practice to routinely examine the data used to calculate the performance metrics to make sure that no unusual behavior goes undetected. Simple graphical tools, such as box plot [16], can be used to obtain a quick assessment on symmetry, concentration, and spread of the data.

Our motivation for developing this algorithm was to create an independent, benchmark method that is both amenable to a thorough uncertainty analysis [9] and can function as a comparison tool since no standardized industry algorithms currently exist. The main advantages of the LMS approach presented here are that we always obtain a unique solution that is insensitive to outliers, data distributions, and small populations. Although we have addressed only the calculation of the parameters and performance metrics of an eye diagram in this paper, we are currently investigating the computation of associated uncertainties and plan to report our findings in a future communication.

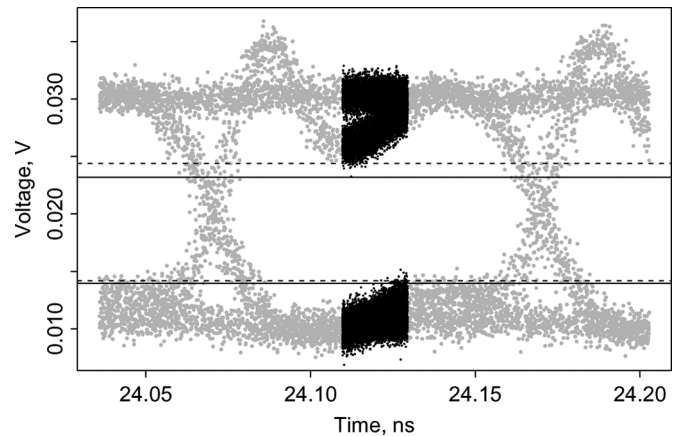


Fig. 12. Data used to calculate eye height for the second setup. The solid lines are mean ± 3 (standard deviation) of the upper and lower clusters, respectively. The dashed lines are the 0.13 and 99.87 percentiles of the upper and lower clusters, respectively.

APPENDIX

We list an R function [17], `eye.pars`, for obtaining fundamental parameters and performance metrics of an eye diagram based on the algorithm described in this paper.

```
eye.pars <- function(xdat, ydat) {
  # INPUT:
  # xdat: vector of time data
  # ydat: vector of voltage data
  #
  # obtain approx center of voltage data
  vm <- mean(kmeans(ydat, 2)$centers)
  # compute shortest interval containing
  # 50% of upper half of voltage data
  top.int <- shorth.int(ydat[ydat > vm])
  # obtain one state
  state.1 <- mean(top.int)
  # compute shortest interval containing
  # 50% of bottom half of voltage data
  bot.int <- shorth.int(ydat[ydat < vm])
  # obtain zero state state.0 <-
  mean(bot.int)
  # obtain amplitude between upper and
  # lower states
  d10 <- state.1 - state.0
  # 75% threshold level
  v75 <- state.1 - 0.25 * d10
  # 25% threshold level
  v25 <- state.0 + 0.25 * d10
  # only consider following time data
  # for finding time crossings
  tt <- xdat[ydat < v75 & ydat > v25]
  # obtain approx center of time data
```

```

tm <- mean(kmeans(tt, 2)$centers)
# compute shortest interval containing
# 50% of left half of time data
leftx.int <- shorth.int(tt[tt < tm])
# obtain left time crossing
left.x <- mean(leftx.int)
# compute shortest interval containing
# 50% of right half of time data
rightx.int <- shorth.int(tt[tt > tm])
# obtain right time crossing
right.x <- mean(rightx.int)
# compute center of eye
t.center <- (left.x + right.x)/2
# form central 20% of the eye diagram
t.dist <- right.x - left.x
t.span0 <- t.center - 0.1 * t.dist
t.span1 <- t.center + 0.1 * t.dist
# within center 20% of eye diagram
# separate voltage data into top and
# base clusters
y.center <- (state.1 + state.0)/2
# obtain top cluster
ycluster.1 <- ydat[ydat > y.center &
(t.span0 < xdat & xdat < t.span1)]
# obtain base cluster
ycluster.0 <- ydat[ydat < y.center &
(t.span0 < xdat & xdat < t.span1)]
# for each cluster, calculate mean and
# standard deviation
vtop.mean <- mean(ycluster.1)
vbase.mean <- mean(ycluster.0)
vtop.sd <- sqrt(var(ycluster.1))
vbase.sd <- sqrt(var(ycluster.0))
# obtain extinction ratio
er <- vtop.mean/vbase.mean
er <- 10 * log10(er)
# obtain eye height
eye.h <- vtop.mean - 3 * vtop.sd -
vbase.mean - 3 * vbase.sd
# compute amplitude values
# corresponding to time crossings
tll <- left.x - 0.01 * t.dist
thh <- left.x + 0.01 * t.dist
amp.dat <- ydat[(ydat < v75 & ydat > v25)
& (tll < xdat & xdat < thh)]
# obtain left crossing amplitude
ampx.1 <- mean(amp.dat)

tll <- right.x - 0.01 * t.dist
thh <- right.x + 0.01 * t.dist
amp.dat <- ydat[(ydat < v75 & ydat > v25)
& (tll < xdat & xdat < thh)]
# obtain right crossing amplitude
ampx.2 <- mean(amp.dat)
# compute RMS jitters
tll <- left.x - 0.25 * t.dist
thh <- left.x + 0.25 * t.dist
tj <- xdat[(ampx.1 - 0.01 * d10 < ydat &
ydat < ampx.1 + 0.01 * d10) & (tll < xdat
& xdat < thh)]
# obtain jitter at left crossing
# amplitude
jitter1 <- sqrt(var(tj))
tll <- right.x - 0.25 * t.dist
thh <- right.x + 0.25 * t.dist
tj <- xdat[(ampx.2 - 0.01 * d10 < ydat &
ydat < ampx.2 + 0.01 * d10) & (tll < xdat
& xdat < thh)]
# obtain jitter at right crossing
# amplitude
jitter2 <- sqrt(var(tj))
# obtain average RMS jitter
jitter <- (jitter1 + jitter2)/2
# obtain eye width eye.w <- right.x - 3 *
jitter2 - left.x - 3 * jitter1
# output includes
# zero state
# one state
# left time crossing
# right time crossing
# extinction ratio
# RMS jitter
# eye height
# eye width
list(state.0 = state.0,
state.1 = state.1,
left.xing = left.x,
right.xing = right.x,
extinction.ratio = er,
jitter = jitter,
eye.height = eye.h,
eye.width = eye.w)
}
#
shorth.int <- function(x) {
# evaluate shortest interval that

```

```

# contains 50% of x
#
nx <- length(x)
if (nx < 2) shi <- c(x, x)
else {
nlag <- nx %/% 2
y <- sort(x)
nz <- nx - nlag
z <- diff(y, lag = nlag)
nn <- (1:nz) [z= min(z)]
ii <- nn
if (length(nn) > 1) ii <- nn[1]
shi <- c(y[ii], y[ii + nlag])
}
shi
}

```

To obtain the results for one of the data sets corresponding to the first setup discussed previously, we first read the data using the following commands:

```

> setup1 <- scan("setup102.dat", list (x = 0,
y = 0), sep=",")
> setup1$x <- setup1$x * 10^9

```

The first command reads the file `setup102.dat` that consists of two columns of data separated by a comma. The columns are time (s) and voltage (V) measurements. The second command converts the unit of time from second to nanosecond. We then invoke the function to obtain the fundamental parameters and performance metrics of this example:

```

> eye.pars(setup1$x, setup1$y)
$state.0
[1] 7.2326e-05
$state.1
[1] 0.00138755
$left.xing
[1] 24.11311
$right.xing
[1] 24.21440
$extinction.ratio
[1] 12.22527
$jitter
[1] 0.003533722
$eye.height
[1] 0.001044979
$eye.width
[1] 0.08009017

```

This code is available in electronic form at http://www.boulder.nist.gov/div815/HSM_Project/.

ACKNOWLEDGMENT

The authors would like to thank D. Humphreys and G. Lecheminant for their detailed reviews of this manuscript.

REFERENCES

- [1] D. Derickson, *Fiber Optic Test and Measurement*. Englewood Cliffs, NJ: Prentice-Hall, 1998.
- [2] P. Andersson and K. Akermark, "Accurate optical extinction ratio measurements," *IEEE Photon. Technol. Lett.*, vol. 6, no. 11, pp. 1356–1358, Nov. 1994.
- [3] T. Clement, P. Hale, D. Williams, C. Wang, A. Dienstfrey, and D. Keenan, "Calibration of sampling oscilloscopes with high-speed photodiodes," *IEEE Trans. Instrum. Meas.*, vol. 54, no. 8, pp. 3173–3181, Aug. 2006.
- [4] M. Hart, C. Duff, and S. Hinch, "Firmware measurement algorithms for the HP83480 digital communications analyzer," *Hewlett-Packard J.*, Dec. 1996.
- [5] W. Finke, "Algorithm for Finding the Eye Crossing Level of a Multi-level Signal," U.S. patent 6,614,434 B1, Sep. 2003.
- [6] *IEEE Standard on Transitions, Pulses, and Related Waveforms*, IEEE Std. 181-2003, Institute of Electrical and Electronics Engineers, Jul. 2003.
- [7] P. Rousseeuw and A. Leroy, *Robust Regression and Outlier Detection*. New York: Wiley, 2004.
- [8] J. A. Hartigan, *Clustering Algorithms*. New York: Wiley, 1975.
- [9] P. D. Hale and C. M. Wang, "Measurement of pulse parameters and propagation of uncertainty," *IEEE Trans. Instrum. Meas.*, to be published.
- [10] J. Gowar, *Optical Communication Systems*. Englewood Cliffs, NJ: Prentice-Hall, 1984.
- [11] OFSTP-4A: Optical Eye Pattern Measurement Procedure, Telecommunications Industries of America/Electronics Industries of America (TIA/EIA) Standard, Nov. 1997.
- [12] IEC 61280-2-2: Fibre Optic Communication Subsystem Test Procedures—Part 2-2: Digital Systems—Optical Eye Pattern, Waveform, and Extinction Ratio Measurement, International Electrotechnical Commission, Apr. 2005.
- [13] GR-253-CORE: Synchronous Optical Network (SONET) Transport Systems: Common Generic Criteria, Telcordia Technologies, Jan. 1999.
- [14] *CSMA/CD Access Method and Physical Layer Specifications—Amendment: Media Access Parameters, Physical Layers, and Management Parameters for 10 Gb/s Operation*, IEEE Std. 802.3ae, Institute of Electrical and Electronics Engineers, Aug. 2002.
- [15] ITU-T Recommendation G.957: Optical Interfaces for Equipments and Systems Relating to the Synchronous Digital Hierarchy, Telecommunication Standardization Sector of International Telecommunications Union (ITU-T), Mar. 2006.
- [16] J. M. Chambers, W. S. Cleveland, B. Kleiner, and P. A. Tukey, *Graphical Methods for Data Analysis*. New York: Wadsworth, 1983.
- [17] R Development Core Team 2003 R: A Language and Environment for Statistical Computing R Foundation for Statistical Computing. Vienna, Austria, 3-900051-00-3 [Online]. Available: <http://www.R-project.org>



Jeffrey A. Jargon (M'98–SM'01) received the B.S., M.S., and Ph.D. degrees in electrical engineering from the University of Colorado at Boulder in 1990, 1996, and 2003, respectively.

He has been a Staff Member of the National Institute of Standards and Technology (NIST), Boulder, CO, since 1990 and has conducted research in the areas of vector network analyzer calibrations and microwave metrology. He is presently a member of the High-Speed Measurements Project in the Optoelectronics Division. He has published over 50 technical

articles.

Dr. Jargon has received four best paper awards, an URSI Young Scientist Award, and a Department of Commerce Silver Medal Award. He is a member of Tau Beta Pi and Eta Kappa Nu and a registered Professional Engineer in the State of Colorado.



C. M. "Jack" Wang received the Ph.D. degree in statistics from Colorado State University, Boulder, in 1978.

He joined the Statistical Engineering Division of the National Institute of Standards and Technology in 1988. He has published over 70 journal articles. His research interests include statistical metrology and the application of statistical methods to physical sciences.

Dr. Wang is a Fellow of the American Statistical Association (ASA) and the recipient of the Department of Commerce Bronze Medals and several awards from ASA.



Paul D. Hale (SM'01) received the Ph.D. degree in applied physics from the Colorado School of Mines, Golden, in 1989.

He has been with the Optoelectronics Division, National Institute of Standards and Technology (NIST), Boulder, CO, since 1989, where he conducts research on broadband optoelectronic device and signal metrology. His current technical work focuses on extending both time- and frequency-domain optoelectronic measurements to beyond 110 GHz, implementing a novel covariance-based uncertainty

analysis that can be used for both time- and frequency-domain quantities, and disseminating NIST traceability through high-speed electronic and optoelectronic measurement services. He has been Leader of the High-Speed Measurements Project in the Sources and Detectors Group since 1996. He has published over 50 technical publications.

Dr. Hale was an Associate Editor of Optoelectronics/Integrated optics for the IEEE JOURNAL OF LIGHTWAVE TECHNOLOGY from June 2001 until March 2007. He has received the Department of Commerce Bronze, Silver, and Gold awards, two ARFTG Best Paper Awards, and the NIST Electrical Engineering Laboratory's Outstanding Paper Award.